Arch. Metall. Mater. **69** (2024), 4, 1467-1472

DOI: https://doi.org/10.24425/amm.2024.151416

G. DERCZ[1*], I. MATUŁA[1], K. PRUSIK[1], J. ZAJĄC[1], M. SZKLARSKA[1],
A. KAZEK-KĘSIK[2], W. SIMKA[2]

EFFECT OF Nb AND Zr ALLOYING ADDITIVES ON STRUCTURE AND PROPERTIES OF Ti-Ta-Nb-Zr ALLOYS FOR MEDICAL APPLICATIONS

This work investigated two titanium-based alloys with a constant tantalum content and variable contents of alloy additives – niobium and zirconium. The Ti-30Ta-10Zr-20Nb (wt.%) and Ti-30Ta-20Zr-10Nb (wt.%) alloys were obtained using a combination of powder metallurgy and arc melting methods. The influence of alloying additives on the structure and properties of the Ti-Ta-Nb-Zr system was studied using, among others: X-ray diffraction and scanning electron microscopy. The X-ray diffraction confirmed the single-β-phase structure of both alloys. In addition, the microscopic analysis revealed that a higher amount of zirconium favoured the formation of larger grains. However, the microhardness analysis indicated that the alloy with the higher niobium content had the higher microhardness. Importantly, the in vitro corrosion study revealed that the addition of niobium promoted the better corrosion resistance of the investigated alloy.

Keywords: Titanium-based alloys; corrosion resistance; biomaterials; arc-melting; structure

1. Introductions

The development of medicine and engineering has enabled the creation and advancement of biomaterials that can be used as implants. There are a number of requirements related to using the material in a living organism. The ideal material for medical applications should have excellent corrosion resistance, full biocompatibility and appropriate mechanical properties. It should not be toxic or mutagenic to the body and should not cause allergies. The most promising biomaterials for medical applications are titanium alloys. The interest in titanium as a biomaterial results from: its mechanical properties similar to human bones, high resistance to corrosion in aggressive environments, high melting point, non-magneticity, osseointegration properties, and biological inertness, which are essential when using Ti for implants. Titanium and its alloys are endowed with the high corrosion resistance due to an oxide layer forming on their surface. It is often a layer of TiO_2 (but also Ti_2O_3 or TiO) [1-7].

When considering titanium alloys as a biomaterial, great attention should be paid to alloying additives which, should ensure both appropriate mechanical properties and high biocompatibility. A proper selection of alloying elements is critical due to the toxic ions release into the body and consequent long-term health problems. Currently, concerns are raised about the cytotoxic effect of vanadium which causes allergies and neurogenic disorders. Studies have also proven the negative impact of aluminium on the nervous system, linking it with the Alzheimer's disease [8-10]. Nickel is also considered a cytotoxic, carcinogenic, and allergenic element [11-13]. Therefore, attempts are being made to replace these alloying elements with other elements that do not show harmful effects in contact with the human body. The most promising alternatives are vital elements such as Nb and Ta which additionally stabilize the β phase. [14-16]

The previous study [17] showed that the Ti-10Ta-10Nb alloy has a higher corrosion resistance than the Ti-6Al-4V alloy. Moreover, niobium as an alloying additive increases the hardness of the alloy [18-20]. Tantalum also is an element that presents excellent biocompatibility and prevents the corrosion products appearance in body fluids. It is characterized by low cytotoxicity, does not cause allergies, and is not genotoxic or mutagenic [21,22]. It was also noticed that the addition of Zr to Ti-Nb alloys might increase the critical stress in the phenomenon of slip and shape memory effect [23]. Furthermore, as an alloying additive, it gives hardness and ductility to alloys.

[1] UNIVERSITY OF SILESIA IN KATOWICE, INSTITUTE OF MATERIALS ENGINEERING, 75 PUŁKU PIECHOTY STR. 1 A, 41-500 CHORZÓW, POLAND
[2] SILESIAN UNIVERSITY OF TECHNOLOGY, FACULTY OF CHEMISTRY, B. KRZYWOUSTEGO STR. 6, 44-100 GLIWICE, POLAND

* Corresponding author: grzegorz.dercz@us.edu.pl

This work investigated two titanium-based alloys with a constant tantalum content and a variable content of alloy additives – niobium and zirconium. The Ti-30Ta-10Zr-20Nb (wt.%) and Ti-30Ta-20Zr-10Nb (wt.%) alloys were obtained using a combination of powder metallurgy and arc melting methods. The additions influence on the structure and properties of the Ti-Ta-Nb-Zr system alloys was studied via X-ray diffraction, scanning electron microscopy, and electrochemical measurements to determine their corrosion resistance.

2. Materials and method

The nominal Ti-30Ta-10Zr-20Nb (wt.%) and Ti-30Ta-20Zr-10Nb (wt.%) composition were prepared using commercial powders: Ti (Atlantic Equipment Engineers (AEE); purity 99.7%, particle size <20 μm), Ta (Sigma Aldrich; purity 99.9%; particle size <9 μm), Zr (Atlantic Equipment Engineers (AEE); purity 99.5%; particle size <300 μm) and Nb (Atlantic Equipment Engineers (AEE), purity 99.8%, particle size <5 μm). The materials were prepared by high-energy milling in the Fritsch Pulverisette 7 premium line planetary ball equipped with a container and milling balls made of hardened steel. The homogenization process was carried out for 24 hours at the rotational speed of 100 rpm, and the ball-to-powder weight ratio was 10:1 under the Ar protective-gas atmosphere. Green compacts from the as-blended powders of 10 mm diameter were compacted under the isostatic pressure of 1000 MPa. The as-pressed green compacts were subjected to a vacuum arc melting (VAM) technique in the Ar atmosphere. The obtained VAM buttons were flipped over and re-melted three times to ensure the homogeneity of chemical compositions.

The phase composition and crystal structure of the obtained materials were studied using the X-ray diffraction method (XRD) performed using the Phillips X-ray X'Pert diffractometer with a lamp with a copper anode ($\lambda_{CuK\alpha}$ – 1.54178 Å) at the 30 mA electric current and 40 kV voltage. The wavelengths emitted from the copper anode were passed through a curved graphite monochromator. The powder diffraction patterns were recorded by scanning at steps of 0.04 over the angular range of 20-150° 2θ.

The scanning electron microscope (SEM) microstructure analysis was performed using the JEOL JSM-6480 (JEOL Ltd., Tokyo, Japan), working with the accelerating voltage of 20 kV and equipped with the energy-dispersive X-ray spectroscopy (EDS) IXRF detector (IXRF, Austin, TX, USA). The microstructure of the samples was also examined using the OLYMPUS metallographic microscope, type GX-51.

The microhardness measurements were carried out using the 401/402 MVD digital microhardness tester manufactured by ITW Test & Measurement equipped with the ~136° pyramidal Vickers tip, under the load of 500 N and dwell time of 10 s.

The electrochemical measurements were carried out using the PARSTAT 4000 (AMETEK) potentiostat. The thermostatic, three-electrode electrochemical cell was used where the studied materials were the working electrode (WE). The Pt mesh was used as a counter electrode (CE), and the saturated calomel electrode (SCE) with the Haber-Luggin capillary was the reference electrode (RE). The in vitro corrosion resistance of the studied materials was investigated in the Ringer's solution (8.6 g/L NaCl, 0.3 g/L KCl, 0.48 g/L CaCl × $6H_2O$) deaerated with argon (Ar, 99.999%) at 37(1)°C. During the measurements, the open circuit potential (E_{OC}), potentiodynamic polarization curve, and cyclic voltammetry curve at a sweep rate of $v = 10$ mV s^{-1}, were registered.

3. Result and discussion

The qualitative phase analysis performed via the X-ray diffraction showed the presence of the β phase of titanium in the Ti-30Ta-20Zr-10Nb alloy (Fig. 1) and the Ti-30Ta-10Zr-20Nb alloy (Fig. 2). The differences in the diffraction lines intensities observed in the X-ray patterns, especially seen in Fig. 2, may be due to the texture and the large grain presence. The formation of a preferential orientation and the possible large grain formation was typical of VAM, which was confirmed by further investigations.

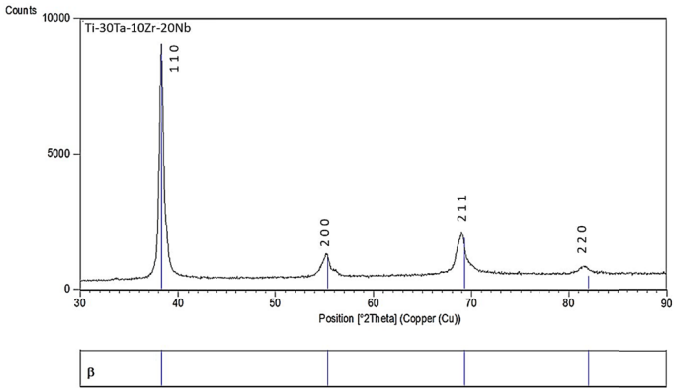

Fig. 1. X-ray diffraction patterns of Ti-30Ta-10Zr-20Nb

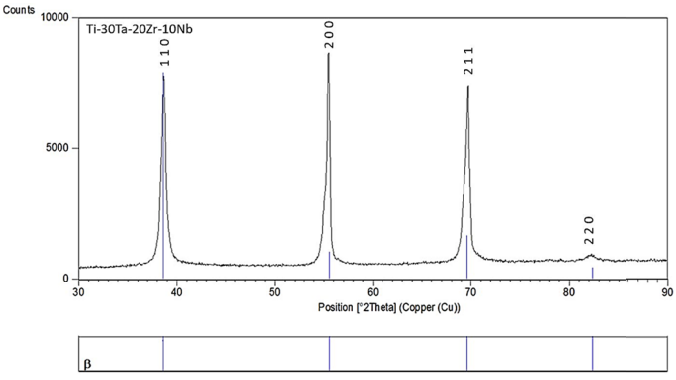

Fig. 2. X-ray diffraction patterns of Ti-30Ta-20Zr-10Nb

The Rietveld method determined lattice parameters for the tested samples (TABLE 1). A significant increase in the lattice parameter a_0 was found. A greater increase was noted for the sample containing more niobium, which confirms the role of niobium as a stabilizer of the β phase. The studies showed that the increase in lattice parameters of the newly formed β phase was

associated with the atomic radius of the alloying elements larger than Ti (1.40 Å), i.e., Zr (1.55Å), Ta (1.45Å) and Nb (1.45Å).

TABLE 1

List of lattice parameters determined by the Rietveld method

Phase	Lattice parameter / nm			
		ICDD*	Rietveld	
			Ti-30Ta-10Zr-20Nb	Ti-30Ta-20Zr-10Nb
β	a_0	0.3307	0.3341(4)	0.3326(5)

* ICDD – The International Center for Diffraction Data

The results of observing the microstructure of the two studied alloys are shown in Fig. 3. In both cases, a single-phase structure was visible. It is also noted that in both cases the grains had a globular shape. The structure of the Ti-30Ta-20Zr-10Nb alloy (Fig. 3b) was finer than that of the Ti-30Ta-10Zr-20Nb alloy (Fig. 3a), due to the lower zirconium content. Due to the high similarity of unit cells in the lattice parameters and the identical space groups of Ta, Nb and β-Ti phases, it can be assumed that the presence of Zr dictated the grain growth. The fine grain size related not only to the reduced Zr content, but also to the slow diffusion rate of the Ti-Ta and Ti-Nb alloys, which was retarded by the alloying addition of: Ta and Nb, respectively. Also, the

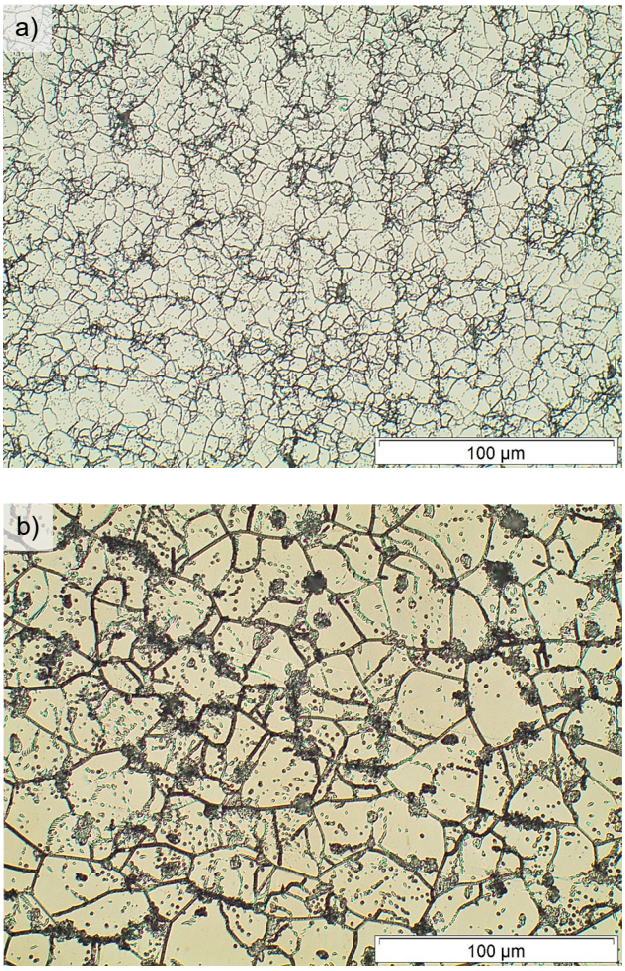

Fig. 3. Optical microscopy images a) for the Ti-30Ta-10Zr-20Nb (wt.%) sample, b) for the Ti-30Ta-20Zr-10Nb (wt.%) sample

observed differences in microhardness for the presented compositions may be related to the materials microstructures. In Fig. 3, much smaller grains were observed for theTi-30Ta-10Zr-20Nb (wt.%) composition which revealed the higher microhardness.

The SEM analysis confirmed the similar and single-phase character of the two tested alloys, manifested by the grain microstructure similar size and shape. The lack of precipitates at the grain boundaries also indicated the single-phase character of the alloys. Fig. 4 shows the fine-grained nature of the microstructure with the clear grain boundaries with a small number of pores. What is essential is that no precipitates of another phase were observed. The SEM analysis of the samples revealed a hierarchical structure of the alloys, i.e. the smaller grains were contained in the larger grains (Fig. 4).The grains in the Ti-30Ta-20Zr-10Nb were larger than in the Ti-30Ta-10Zr-20Nb, due to the greater zirconium content responsible for the grain enlargement.

The grain surface areas were calculated using the planimetric method (TABLE 2). The obtained results showed that the grains in the Ti-30Ta-20Zr-10Nb sample were twice as large as in Ti-30Ta-10Zr-20Nb. The factor determining the number of grains per unit area (N_A) was 7080 mm^{-2} and 34342 mm^{-2} for Ti-30Ta-20Zr-10Nb and Ti-30Ta-10Zr-20Nb, respectively. Moreover, the value of the elongation factor was higher in the Ti-30Ta-10Zr-20Nb sample. The upper limit of the circularity coefficient was 1, which indicated a globular grain shape. The Ti-30Ta-10Zr-20Nb sample had a higher value of the circularity coefficient, which indicated a much more globular shape of the grains compared to the Ti-30Ta-20Zr-10Nb alloy.

TABLE 2

Parameters obtained by planimetric grain analysis

	a / µm^2	v	f_1	f_2	N_A / mm^{-2}
Ti-30Ta-10Zr-20Nb	28.122	1.060	1.148	0.481	34342
Ti-30Ta-20Zr-10Nb	73.688	1.505	1.329	0.358	7080

The EDS detector registered the distribution maps (Fig. 5) of the elements during the SEM observation for the tested samples. Fig. 5 shows an even distribution of elements, which proves the alloys homogeneity. The shadows visible in the case of Zr and Nb resulted from the etching process of the sample.

For the Ti-30Ta-10Zr-20Nb sample, the average HV0.5 microhardness value was 432(11), while for the Ti-30Ta-20Zr-10Nb sample, it was 384(12). The sample with the higher Nb content and the lower Zr content was characterized by the higher hardness. Both zirconium and niobium are elements that increase the alloy hardness. In the studies carried out by Takahashi in [24], it was shown that the alloy hardness increased with the zirconium content in the binary Ti-Zr alloys. Our performed tests did not confirm this, probably due to the plastic tantalum, the very fine microstructure, and the solid-solution strengthening. In addition, according to the commonly accepted point of view, the reduced hardness of Ti-Ta alloys is explained by a decrease in the ω phase amount present in them. In our case, the ω phase was absent in the structure of the studied alloys. Therefore, the most likely

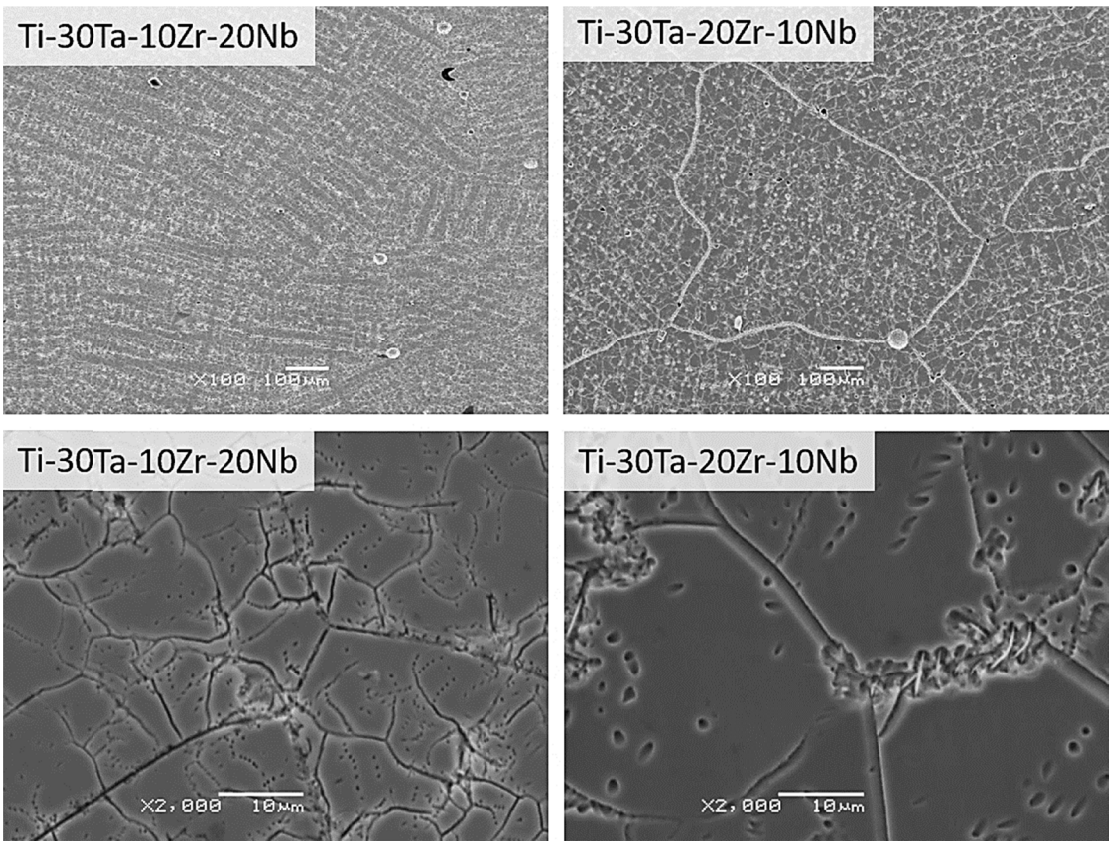

Fig. 4. SEM micrographs of the Ti-30Ta-10Zr-20Nb and Ti-30Ta-20Zr-10Nb samples

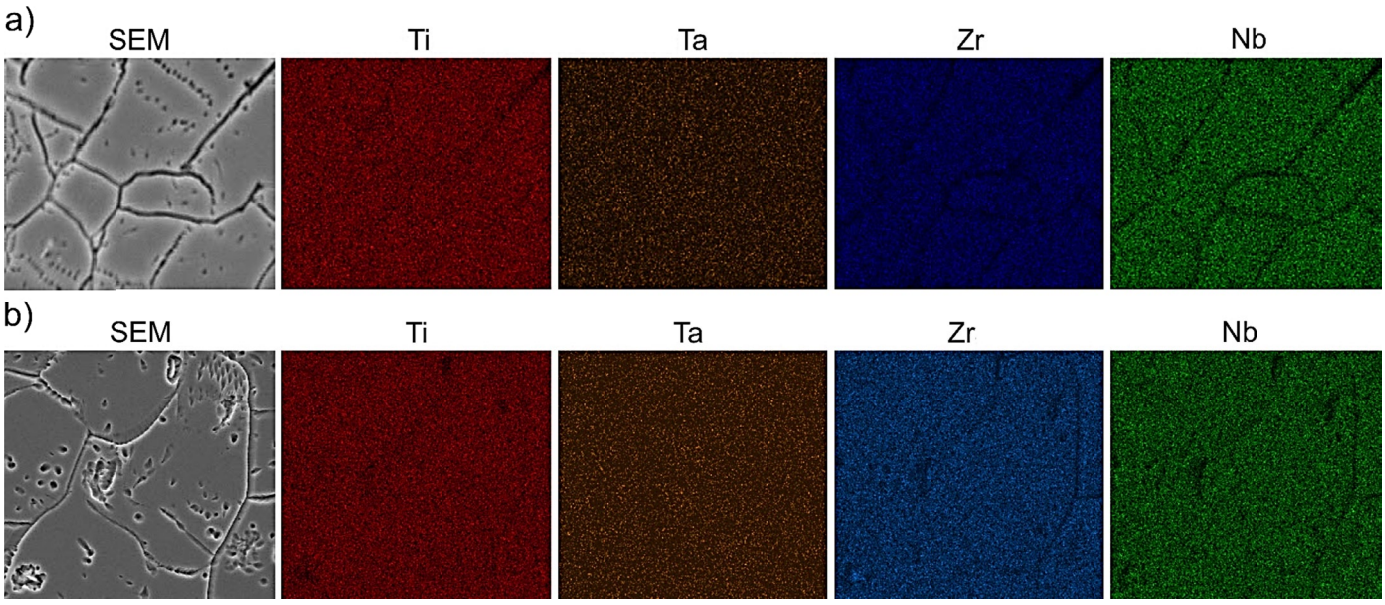

Fig. 5. Distribution maps of the elements for the a) Ti-30Ta-10Zr-20Nb (wt.%), b) Ti-30Ta-20Zr-10Nb

reason for the slight reduction in hardness, despite the presence of Zr in the concentration range of about 30 wt.%, is that Ti-Ta alloys exhibit a shape memory effect in this range. In addition, the presence of niobium may also promote the formation of alloys with shape memory [25].

Also, the observed microhardness differences of the investigated compositions may be related to the materials microstructure and the Hall-Petch relationship. In Fig. 3, the much smaller grains were observed for the composition Ti-30Ta-10Zr-20Nb (wt.%) which revealed the higher microhardness.

TABLE 2 presents the results of the corrosion resistance tests for the tested titanium alloys in the Ringer's solution. In the in vitro studies, the E_{OC} measurements were carried out for 60 min until the ionic-electron equilibrium related to the double electrical layer formation at the electrolyte/oxide layer interface was stabilized. The E_{OC}'s registered value was higher for the

TABLE 3

Summary of corrosion resistance measurements results

	E_{OC} / mV	E_{COR} / mV	R_p / Ω cm^2	j_{COR} / A cm^{-2}	β_a	β_b
Ti-30Ta-10Zr-20Nb	–258.8	–276.1	$1.0 \cdot 10^7$	$4.3 \cdot 10^{-8}$	0.269	0.446
Ti-30Ta-20Zr-10Nb	–141.7	–97.2	$1.7 \cdot 10^6$	$2.6 \cdot 10^{-7}$	0.188	0.120

Ti-30Ta-20Zr-10Nb sample and reached –141.7 mV, whereas, for Ti-30Ta-10Zr-20Nb, E_{OC} was equal to –258.8 mV. The higher polarization resistance value (R_p), $1.0 \cdot 10^7$ Ω cm^2, characterized the Ti-30Ta-10Zr-20Nb sample. Also, a slightly lower corrosion current density value ($j_{COR} = 4.3 \cdot 10^{-8}$ A·cm^{-2}) was determined for this alloy. For the Ti-30Ta-20Zr-10Nb sample, the polarization resistance value was $1.7 \cdot 10^6$ Ω·cm^2, and the current density increased to $2.6 \cdot 10^{-7}$ A·cm^{-2}. Those results show that the determined corrosion parameters vary, depending on the Zr and Nb content in the studied Ti alloys. The results also proved the Ti-30Ta-10Zr-20Nb slightly better corrosion resistance.

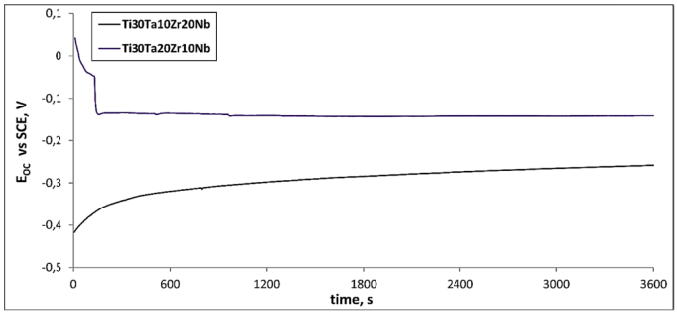

Fig. 6. Open circuit potential as a function of time for the Ti-30Ta-10Zr-20Nb and Ti-30Ta-20Zr-10Nb electrodes in Ringer's solution at 37°C

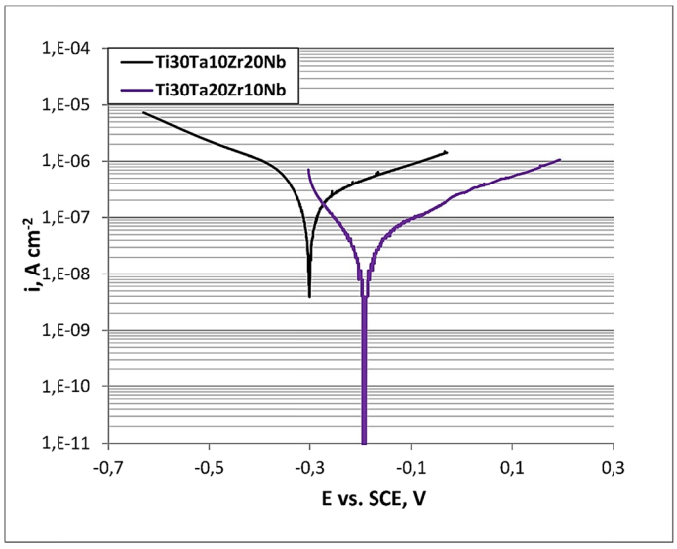

Fig. 7. Anodic polarization curves for the Ti-30Ta-10Zr-20Nb and Ti-30Ta-20Zr-10Nb electrodes in Ringer's solution with different pH at 37°C

The obtained voltametric curves were characteristic of titanium alloys. For both titanium alloys, the current density values increased above the 0.4 V vs. SCE potential. An intensive increase in the current density was observed at the 1.2 V vs. SCE potential and reached its maximum around the 2.5 V potential. The shape of the voltametric curves indicated the formation of oxide layers on the sample surfaces. First, the titanium oxides such as TiOOH, and Ti_2O_3 were formed. Then at the potential above 0.1 V, the Ti^{3+} ions were oxidized to Ti^{4+}, creating the stable TiO_2 form. The recorded signal at the 1.4-2 V vs. SCE potential indicated the electrode oxidation and the alloy oxides formation , including non-stoichiometric oxides. The Ti-30Ta-20Zr-10Nb sample revealed the higher current density than the Ti-30Ta-10Zr-20Nb one. The content of niobium, an element characterized by high corrosion resistance, may impact the decrease in the current density value.

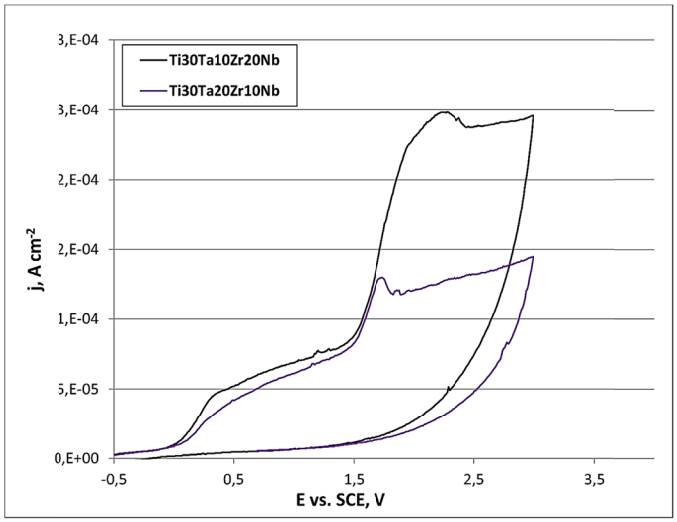

Fig. 8. Voltametric curves for the Ti-30Ta-10Zr-20Nb and Ti-30Ta-20Zr-10Nb electrodes in Ringer's solution with different pH at 37°C

The obtained results are in good agreement with the literature data. Karayan et al. [17] compared the corrosion resistance of titanium alloys with different contents of niobium and tantalum (Ti-8Ta-3Nb and Ti-10Ta-10Nb) with the corrosion resistance of technical titanium and the Ti-6Al-4V alloy. The research shows that the best corrosion resistance characterizes the alloys with the highest amount of niobium, which is related to the reduction of the passive current density and shifting the corrosion potential in the noble direction.

4. Conclusions

The research showed that it was possible to obtain the four-component alloys, Ti-30Ta-10Zr-20Nb (wt.%) and

Ti-30Ta-20Zr-10Nb (wt.%), with the single-β-phase structure by the vacuum arc melting (VAM) technique. The elements distribution maps proved an even distribution of all the elements in the obtained material. The microscopic analysis revealed that a higher amount of zircon favoured the formation of larger grains. However, the microhardness analysis indicated that the alloy with the higher niobium content was found to have the higher microhardness. The electrochemical measurements revealed that adding niobium promoted better corrosion resistance of the alloy.

REFERENCES

[1] M. Geetha, A.K. Singh, R. Asokamani, A.K. Gogia, Ti based biomaterials, the ultimate choice for orthopaedic implants – A review. Prog. Mater. Sci. **54**, 3, 397-425 (2009). DOI: https://doi.org/10.1016/j.pmatsci.2008.06.004

[2] K. Wang, The use of titanium for medical applications in the USA. Mater. Sci. Eng. A **213**, 1-2, 134-137, Aug. (1996). DOI: https://doi.org/10.1016/0921-5093(96)10243-4

[3] Y. Li, C. Yang, H. Zhao, S. Qu, X. Li, Y. Li, New developments of ti-based alloys for biomedical applications. Materials (Basel). **7**, 3, 1709-1800 (2014). DOI: https://doi.org/10.3390/ma7031709

[4] M. Szklarska, G. Dercz, J. Rak, W. Simka, B. Losiewicz, The influence of passivation type on corrosion resistance of Ti15Mo alloy in simulated body fluids. Arch. Metall. Mater. **60**, 4, 2687-2693 (2015). DOI: https://doi.org/10.1515/amm-2015-0433

[5] M. Szklarska, G. Dercz, W. Simka, B. Łosiewicz, A.c. impedance study on the interfacial properties of passivated Ti13Zr13Nb alloy in physiological saline solution. Surf. Interface Anal. **46**, 10-11, 698-701 (2014). DOI: https://doi.org/10.1002/sia.5383

[6] W. Simka et al., Modification of a Ti-Mo alloy surface via plasma electrolytic oxidation in a solution containing calcium and phosphorus. Electrochim. Acta **96**, 180-190 (2013). DOI: https://doi.org/10.1016/j.electacta.2013.02.102

[7] I. Matuła et al., Microstructure and porosity evolution of the Ti–35Zr biomedical alloy produced by elemental powder metallurgy. Materials (Basel) 2020). DOI: https://doi.org/10.3390/ma13204539

[8] J. Willis, S. Li, S.J. Crean, F.N. Barrak, Is titanium alloy Ti-6Al-4 V cytotoxic to gingival fibroblasts – A systematic review. Clinical and Experimental Dental Research (2021). DOI: https://doi.org/10.1002/cre2.444

[9] K.J. Bozic, S.M. Kurtz, E. Lau, K. Ong, D.T.P. Vail, D.J. Berry, The epidemiology of revision total hip arthroplasty in the United States. J. Bone Joint Surg. Am. **91**, 1, 128-133, Jan. (2009). DOI: https://doi.org/10.2106/JBJS.H.00155

[10] S. Rao, T. Ushida, T. Tateishi, Y. Okazaki, S. Asao, Effect of Ti, Al, and V ions on the relative growth rate of fibroblasts (L929) and osteoblasts (MC3T3-E1) cells. Biomed. Mater. Eng. **6**, 2, 79-86 Accessed: Jun. 20, 2017. [Online]. Available: http://www.ncbi.nlm.nih.gov/pubmed/8761518

[11] K.S. Cameron, V. Buchner, P.B. Tchounwou, Exploring the molecular mechanisms of nickel-induced genotoxicity and carcinogenicity: A literature review. Rev. Environ. Health (2011). DOI: https://doi.org/10.1515/reveh.2011.012

[12] E. Denkhaus, K. Salnikow, Nickel essentiality, toxicity, and carcinogenicity. Critical Reviews in Oncology/Hematology (2002). DOI: https://doi.org/10.1016/S1040-8428(01)00214-1

[13] S. Buxton et al., Concise review of nickel human health toxicology and ecotoxicology. Inorganics (2019). DOI: https://doi.org/10.3390/inorganics7070089

[14] H.J. Rack, J.I. Qazi, Titanium alloys for biomedical applications. Mater. Sci. Eng. C, (2006). DOI: https://doi.org/10.1016/j.msec.2005.08.032

[15] A.M. Khorasani, M. Goldberg, E.H. Doeven, G. Littlefair, Titanium in biomedical applications – properties and fabrication: A review. Journal of Biomaterials and Tissue Engineering (2015). DOI: https://doi.org/10.1166/jbt.2015.1361

[16] G. Dercz, I. Matuła, M. Zubko, J. Dercz, Phase composition and microstructure of new Ti-Ta-Nb-Zr biomedical alloys prepared by mechanical alloying method. Powder Diffr. **32**, S1, S186-S192 (2017). DOI: https://doi.org/10.1017/S0885715617000045

[17] A.I. Karayan, S.W. Park, K.M. Lee, Corrosion behavior of Ti-Ta-Nb alloys in simulated physiological media. Mater. Lett. (2008). DOI: https://doi.org/10.1016/j.matlet.2007.10.028

[18] M.K. Han, J.Y. Kim, M.J. Hwang, H.J. Song, Y.J. Park, Effect of Nb on the microstructure, mechanical properties, corrosion behavior, and cytotoxicity of Ti-Nb alloys. Materials (Basel). (2015). DOI: https://doi.org/10.3390/ma8095287

[19] Y. Guo, K. Georgarakis, Y. Yokoyama, A.R. Yavari, On the mechanical properties of TiNb based alloys. J. Alloys Compd. **571**, 25-30 (2013). DOI: https://doi.org/10.1016/j.jallcom.2013.03.192

[20] T. Tian, B. Dang, F. Li, K. Yang, D. Wei, P. Zhang, Microstructure, mechanical and antibacterial properties of TiNb-based alloy implanted by silver ions. Coatings (2021). DOI: https://doi.org/10.3390/coatings11101213

[21] A. Biesiekierski, J. Wang, M. Abdel-Hady Gepreel, C. Wen, A new look at biomedical Ti-based shape memory alloys. Acta Biomater. **8**, 5, 1661-1669 (2012). DOI: https://doi.org/10.1016/j.actbio.2012.01.018

[22] E. Delvat, D.M. Gordin, T. Gloriant, J.L. Duval, aM.D. Nagel, Microstructure, mechanical properties and cytocompatibility of stable beta Ti-Mo-Ta sintered alloys. J. Mech. Behav. Biomed. Mater. **1**, 4, 345-351 (2008). DOI: https://doi.org/10.1016/j.jmbbm.2008.01.006

[23] X.H. Zheng et al., Thermal stability and high-temperature shape memory effect of Ti-Ta-Zr alloy. Scr. Mater. **68**, 12, 1008-1011, (2013). DOI: https://doi.org/10.1016/j.scriptamat.2013.03.008

[24] M. Takahashi, M. Kikuchi, O. Okuno, Grindability of Dental Cast Ti-Zr Alloys. Materials Transactions **50**, 4, 859-863 (2009). DOI: https://doi.org/10.2320/matertrans.MRA2008403

[25] A.V. Dobromyslov, G.V. Dolgikh, Y. Dutkevich, T.L. Trenogina, Phase and structural transformations in Ti-Ta alloys. Phys. Met. Metallogr. **107**, 5, 502-510, May (2009). DOI: https://doi.org/10.1134/S0031918X09050111/metrics